J Mater Sci: Mater Med (2009) 20:799–808
DOI 10.1007/s10856-008-3636-6

Collagen–chitosan polymer as a scaffold for the proliferation of human adipose tissue-derived stem cells

Yanxia Zhu · Tianqing Liu · Kedong Song · Bo Jiang · Xuehu Ma · Zhanfeng Cui

Received: 11 July 2008 / Accepted: 16 October 2008 / Published online: 20 November 2008

Abstract The architecture and biomaterial are vital for three-dimensional culture of cells in scaffolds, so collagen–chitosan scaffolds suitable for the proliferation of adipose tissue-derived stem cells (ADSCs) were fabricated in this study. Chitosan was fully mixed with collagen with different volume ratio and cross-linked. The microstructure, pore size, bibulous ability, water content, interval porosity, enzyme degradation and affinity were examined before and after cross-linking. During ADSCs cultured in scaffold, the viability and metabolic rates were measured. After 14 days, the surface markers, specific transcription factors and multi-differentiation potential were assayed to identify the stemness of expanded cells. According to the pore size, bibulous ability, interval porosity, degradation rate and affinity of the scaffold, we chose cross-linked scaffolds of 7:3 material ratio as a better scaffold for ADSCs proliferation, and ADSCs could be expanded by more than 20 times. All expanded cells still maintained stem cell characteristics and pluripotency. So our developed collagen–chitosan scaffolds can promote ADSCs adhesion, expansion, and maintain pluripotency.

Y. Zhu · T. Liu (✉) · K. Song · B. Jiang · X. Ma
Dalian R&D Center for Stem Cell and Tissue Engineering, Dalian University of Technology, Liaoning, Dalian 116024, China
e-mail: liutq@dlut.edu.cn

Z. Cui
Department of Engineering Science, Oxford Centre for Tissue Engineering and Bioprocessing, Oxford University, Oxford OX1 3PJ, UK

1 Introduction

A cell-based tissue engineering technique has been proved to be one of the most promising alternative therapies for regenerative medicine. This approach consists of an interactive triad of responsive cells, supportive matrix, and bioactive molecules promoting differentiation and regeneration [1]. Stem cell will be a promising cell for its renewable ability and multipotential. In recent years, interest has rapidly grown in the developmental plasticity and therapeutic potential of stromal cells isolated from adipose tissue, called adipose tissue-derived stem cell (ADSC). Therefore, adipose tissue represents an abundant, practical, and appealing source of donor tissue for autologous cell replacement and tissue engineering. ADSC will play a prominent role in the context of regenerative medicine.

However, the static amplification of stem cells is a time-consuming procedure and prone to contamination [2]. The increasing clinical applications appeal for an alternative to rapidly expand stem cells [3]. In the previous study, we have demonstrated that our isolated ADSC can be easily harvested and expanded rapidly and permanently (three logarithmic phase in one month) without losing their multiple mesenchymal-lineage differentiation potentials [4]. After the cell slice formed however, the slice was rolled and the growth of cells was inhibited, which resulted from the space and nutrient diffusion limitation inside the cell slice.

In contrast, inside a tissue structure, the extracellular matrix (ECM) could provide tissues with the appropriate three-dimensional (3D) architecture, ECM molecules also influence cell migration, proliferation, and differentiation through cell–cell and cell–substrate interactions [5, 6]. Such a complex biological microenvironment does not

exist in traditional two-dimensional (2D) tissue culture plates. To mimic this 3D growth environment in vitro, a variety of biomaterials have been used as substitutes for ECM, providing a physical support matrix and increasing cell–cell and cell–substrate interactions [5, 7]. Bioengineered scaffolds have been introduced to provide a microenvironment that facilitates cell proliferation and differentiation [8, 9]. It is therefore necessary to construct biomimetic scaffolds that improve the interactions between the scaffolds and cells.

Collagen as one of exocellular matrixes has well-documented structural, chemical and physical properties, low antigenicity, good biocompatibility, and the ability to promote cell attachment and proliferation [10–12]. Mesenchymal stem cells were cultured on a collagen scaffold and differentiated into osteocytes [13]; ADSCs were also cultured in collagen scaffold and differentiated into other cells [14, 15]; and Collagen I gel can facilitate homogenous bone formation of ADSCs in PLGA-beta-TCP scaffold [16].

However, the fast biodegrading rate and the low mechanical strength of the untreated collagen scaffold are the crucial problems that limit the further use of this material [17]. Chitosan with high mechanical strength on the other hand has been proved to be biologically renewable, biodegradable, biocompatible, non-antigenic and non-toxic, and recognized as prominent biomaterials [11, 18].

Nevertheless, the rigid crystalline structure makes them hard to dissolve in water, which has retarded their potential for application in the biological field [18, 19]. So combining collagen and chitosan as a porous scaffold can avoid the disadvantage of two materials.

The applications of porous collagen–chitosan scaffolds for tissue engineering have been reported. Tan et al. [7] demonstrated that the addition of chitosan greatly influenced the ultrastructure of collagen and changed the collagen fiber cross-linking, which reinforced the structure and increased pore size. Variety of collagen–chitosan scaffolds have been fabricated for fibroblasts, chondrocytes and periodontal ligament cells [1, 11, 20, 21]. To date however, there is no report about ADSC response to the collagen–chitosan scaffold.

Herein we describe the fabrication of collagen–chitosan porous scaffold, and the further treatment of the scaffold with EDC cross-linkage. The microstructure, the swelling capacity, as well as the degradability of the collagen–chitosan scaffold were investigated. Then, a better scaffold that has good affinity with ADSC was prepared for the expansion of ADSC. In vitro culture tests of ADSC in plates and in scaffolds demonstrated that the scaffolds can promote the expansion of ADSCs efficiently.

2 Materials and methods

2.1 Fabrication of porous collagen–chitosan scaffolds

Collagen–chitosan composite scaffolds were made by the freeze-drying method. About 0.5% (w/v) type I collagen solution and 2% chitosan solution were prepared in 0.1 M acetic acid. The two solutions were then mixed in the ratios 9:1, 7:3, 5:5, 3:7 and 1:9 (collagen:chitosan, v/v). These mixtures were then frozen at −80°C for 2 h and then lyophilized for 24 h in a freeze dryer (LABCONCO Co., Kansas, MO, USA).

The scaffolds were then cross-linked by carbodiimide (EDC). Briefly, scaffolds with uniform size (15 mm in diameter, 2 mm in thickness) were cross-linked by immersing them in 2 ml of 40% (v/v) ethanol containing 50 mM methyl ethanesulfonate (MES) (pH 5.0), 33 mM EDC and 8 mM *N*-hydroxyl succinimide NHS for 10 h. The scaffold acidity was neutralized with 0.1 M Na_2HPO_4 (pH 9.1) for 1 h. Excess base was then removed by repeated washing with 40% ethanol and distilled water until the matrix pH returned to the physiologic range (7.0–7.4) and then freeze-dried. Cross-linked porous scaffolds were sterilized with ethylene oxide gas, and sufficient period of time was allowed to pass for full release of ethylene oxide gas.

2.2 Scanning electron microscope (SEM) observation

Scaffolds were placed on a copper mount and coated using a gold-coating apparatus. Scaffold morphology was investigated using scanning electron microscope (JEM-1200EX, Japan). Distinct sections from each sample were imaged (4 images per sample), and the pore size was determined using the Image-Pro Plus software analysis system. At least 30 pores were assessed for each sample. Data are presented as mean pore size ± standard error.

2.3 Bibulous ability

The initial weights of scaffolds with same size (1.5 × 1.5 × 0.2 cm) were measured with analytic balance, then penetrated in distilled water until equilibrium. The swollen weights of various scaffolds were accurately determined after removing the water from the surface with filter paper. Bibulous ability and water content of scaffolds were calculated from the formula:

Bibulous ability $X = (W_e - W_0)/W_0$; water content H (%) $= (W_e - W_0)/W_e \times 100\%$, where W_e is the weight of the scaffold at swelling equilibrium, W_0 is the initial weight of the scaffold.

2.4 Interval porosity

The initial weights of scaffolds with same size were examined by analytic balance, and then the scaffolds were soaked in dehydrated alcohol at room temperature for 24 h. After the excess ethanol was wiped from the surface of scaffolds, the scaffolds were weighted once again. Then the interval porosity of collagen–chitosan scaffolds can be calculated according to the following equation:

$$\text{Interval porosity } (\%) = \frac{(W - W_0)\rho_1}{\rho_1 W + (\rho_2 - \rho_1)W_0} \times 100\%$$

where W_0 is the initial weight of the scaffold, W the swollen weight, ρ_1 the average density of collagen–chitosan (1.41 g/ml), and ρ_2 is the density of dehydrated alcohol (0.79 g/ml).

2.5 In vitro enzymatic biodegradability

Enzymatic degradation of collagen–chitosan scaffolds was investigated by monitoring the mass loss of scaffold samples as a function of exposure time to collagenase solution. Each scaffold sample (1.5 × 1.5 × 0.2 cm) was suspended in PBS (pH 7.4) in a shaking water bath at 37°C until the scaffolds became swollen. Then the initial weights of the swollen samples were measured after the excess water was wiped from the surfaces of the scaffolds. The scaffolds were then placed in PBS containing 10 mg/ml collagenase at pH 7.4 and 37°C with gentle shaking. Mass loss of the samples was tracked at 6, 12, 24, 48, 72 h, based on the initial swollen weight. Three specimens were tested for each kind of scaffold. The remaining weight percentage of collagen–chitosan scaffolds was calculated according to the following equation:

$$\text{Residual mass } (\%) = \frac{W_t}{W_0} \times 100\%$$

where W_0 is the initial weight of the swollen scaffold and W_t is the swollen weight of the scaffold at each time point.

2.6 Affinity of ADSC with scaffolds

Human adipose tissue-derived stem cells were isolated with our improved method [4]. ADSCs over passage four were used in experiments. After 100% confluence, the cells were digested by trypsin–EDTA and cell density was adjusted to 1×10^7/ml in culture medium (HG-DMEM + 10% FBS). Based on the porosity and biodegradability etc. properties of the fabricated scaffolds, we selected collagen–chitosan scaffolds in the ratio 7:3 and 5:5 as better scaffolds. The sterilized scaffolds were shaped into 5 × 5 × 1 mm pieces and transferred into 24-well plastic culture plates. After rinsed with sterile PBS for three times and prewetted with culture medium overnight, 10 μl cell suspensions were seeded into each scaffold. After 3 h incubation, the scaffolds were transferred into 96-well culture plate and supplied 100 μl culture medium each well. The culture was set at 37°C in 5% CO_2 humidified atmosphere.

The cells were fixed on scaffold after 7 days of culture and observed by SEM, or stained with hematoxylin–eosin (H&E) for the nucleus and cytoplasm and visualized under microscope.

2.7 ADSC expansion in scaffold

According to the physical and chemical characteristics, as well as affinity with ADSCs, we selected collagen–chitosan scaffold with volume ratio of 7:3 as the best scaffold to ADSCs. Then ADSCs with concentration of 1×10^7/ml were seeded in scaffolds and cultured for 14 days. ADSCs were also seeded in plate as 2D control. The percentage of viable cells was determined by CCK-8 kit every other day; the variation in glucose and lactic acid concentration during the experimental period were analyzed every day. After 14 day expansion, the morphology of cells attached to the scaffold was observed by SEM; surface markers of expanded ADSCs were analyzed by flow cytometry; transcription factors Oct-4, Sox-2 and Rex-1 were examined by reverse transcription polymers enzyme reaction (RT-PCR); multi-differentiation ability of expanded cells was also identified by inducing ADSCs into adipocytes, osteocytes and chondrocytes.

2.8 Statistical analysis

All experiments were performed three times, with each treatment conducted in triplicate. Means and standard error were calculated, and the statistical significance of differences among each group was examined by one-way analysis of variance (ANOVA) and a post hoc *t*-test. The post hoc *t*-test was performed when the ANOVA test indicated significance at the $P < 0.05$ levels.

3 Results

3.1 Microstructure of scaffolds

After lyophilization, all scaffolds showed white color with rough surface. The interior of scaffolds was porosity structure as sponginess. The scaffolds with collagen–chitosan ratio of 9:1 were the most porous, while with the ratio of 1:9 were the most compact. The volume of scaffolds decreased with the decrease of collagen concentration, especially for the scaffolds with collagen–

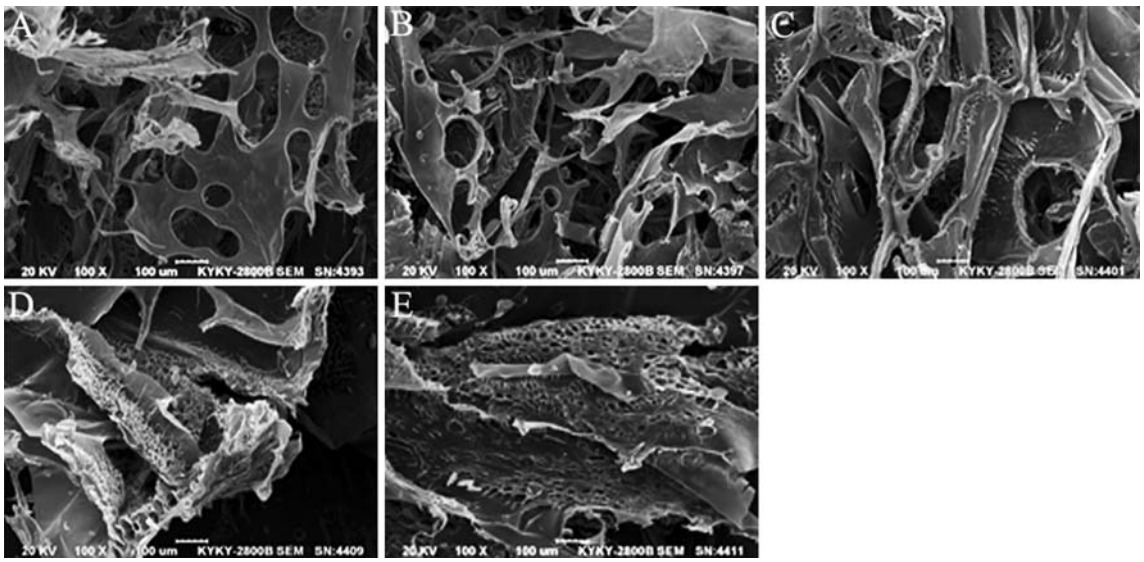

Fig. 1 SEM photographs of non-cross-linked scaffold surface. Volume ratios of collagen–chitosan: **a** 9:1, **b** 7:3, **c** 5:5, **d** 3:7, **e** 1:9

chitosan ratio of 9:1. The cross-section in contact with the mold of collagen scaffolds revealed an interconnected network pore configuration and high porosity throughout the cross-section. As shown in Fig. 1a, collagen–chitosan scaffolds with high concentration of collagen exhibited macroporous microstructure. The pores were interconnected with pore size of about 180 μm, the largest pore size could achieve 300 μm. With the decreasing of collagen concentration, pore size of scaffolds decreased obviously (Table 1). Accompanying with reduction of collagen fibers in between pores, more sheet-like structure appeared together with condensed walls. The interconnected 3D porous structure of the scaffolds was retained after EDC treatment, elongated pores were existed in the cross-linked scaffolds (Fig. 2).

Table 1 The pore size, bibulous ability, water content and interval porosity of scaffolds with different ratios

Volume ratios of collagen–chitosan	Pore diameter (μm)	Bibulous ability (X)	Water content (H%)	Interval porosity (%)
Non-cross-linked				
9:1	103 ± 30	7.24 ± 1.2	87.5 ± 4.3	90.01 ± 0.3
7:3	79 ± 15	11.33 ± 1.5	92.3 ± 3.9	91.21 ± 0.2
5:5	53 ± 11	17.54 ± 2.1	94.6 ± 4.5	90.96 ± 0.4
3:7	22 ± 7	15.51 ± 1.7	92.5 ± 3.7	90.78 ± 0.2
1:9	21 ± 9	11.64 ± 1.1	88.8 ± 2.9	91.25 ± 0.3
Cross-linked				
9:1	154 ± 71	7.87 ± 1.3	89.7 ± 3.8	91.71 ± 0.2
7:3	139 ± 48	10.92 ± 1.3	90.9 ± 4.1	95.22 ± 0.3
5:5	71 ± 29	11.69 ± 1.6	91.5 ± 4.3	93.33 ± 0.4
3:7	29 ± 13	9.14 ± 1.8	90.5 ± 3.9	95.41 ± 0.3
1:9	26 ± 10	8.26 ± 1.2	88.5 ± 2.7	94.12 ± 0.5

3.2 Bibulous ability and interval porosity

From comparative studies of the swelling properties of various scaffolds, scaffolds of 7:3 groups showed maximum bibulous ability of 17.54% in phosphate buffer. After cross-linking, the bibulous ability and water content were lower than those of non-cross-linking. Interval porosity of all scaffolds exceeds 90% (Table 1).

3.3 In vitro biodegradability

The enzymatic degradation of collagen–chitosan scaffolds was investigated by monitoring the residual mass percent of the matrix as a function of time. As shown in Fig. 3, collagen–chitosan scaffolds that were not cross-linked with EDC degraded rapidly, faster than those cross-linked. The residual mass decreased to approximately 55% when cross-linked scaffolds were treated with 10 mg/ml collagenase solution for 6 h, whereas non-cross-linked scaffolds left <50% and almost completely degraded after 72 h. Degradation rate of uncross-linked scaffolds increased with the decrease of collagen density, while that of cross-linked scaffolds decreased.

3.4 The affinity with ADSCs

ADSCs were cultured in the scaffolds with collagen–chitosan volume ratio 7:3 and 5:5. After 1 day cultivation, it showed positive attachment and growth. Finally cells-scaffold structures were observed with SEM. The

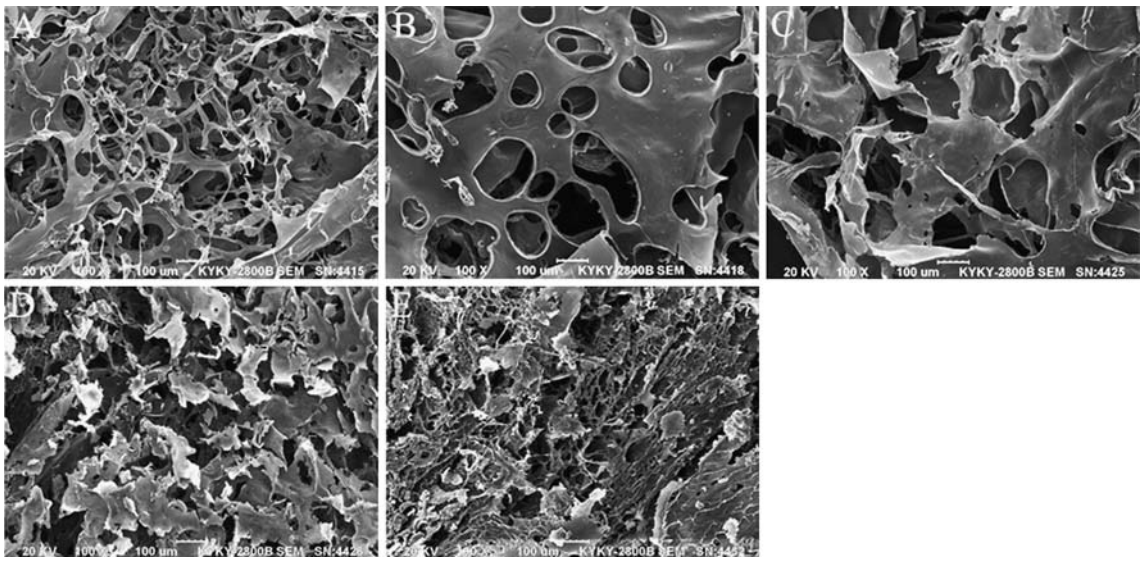

Fig. 2 SEM photographs of cross-linked scaffold surface. Volume ratios of collagen–chitosan: **a** 9:1, **b** 7:3, **c** 5:5, **d** 3:7, **e** 1:9

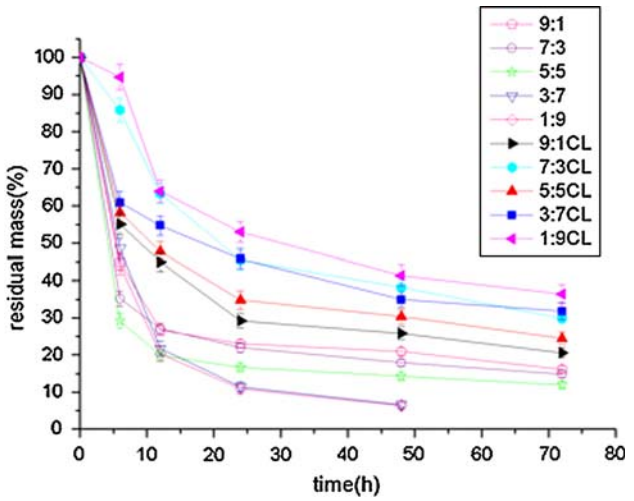

Fig. 3 In vitro enzymatic degradation speed of collagen–chitosan scaffolds with different collagen contents. (Each data point represents the average of three samples)

morphology of ADSCs displayed polygon and grew crawly in scaffolds (Fig. 4a, b). Histology staining of two kinds of scaffolds showed amount of cells presented in the pores and on the surface of scaffold with volume ratio of 7:3, however, there were only a few cells presenting in scaffold of 5:5 after 7 days cultivation (Fig. 4c, d).

3.5 Culture of ADSCs in scaffold

According to the characteristics of scaffolds and biocompatibility with ADSCs, we chose the scaffold with volume ratio of 7:3 as the suitable scaffold for the expansion of ADSCs. The expansion rate of ADSCs in scaffold was higher than that in plate (Fig. 5a). By the end of 14 day culture, the density of cells cultured in plate was nearly 9-fold higher over initial, while almost 20-fold expansion was realized in scaffold (Fig. 5b). We also could see that the ADSCs in scaffolds remained high proliferation rate by the end of experimental period, while in plate, the proliferation of ADSCs was inhibited after 14 days cultivation.

Glucose consumption and lactic acid production of ADSCs in scaffold during the culture time are higher than those in plate. By the end of culture, ADSCs in scaffolds still remained high glucose consumption and lactic acid production (Fig. 6). The metabolic rates were consistent with the growth dynamics of ADSCs in scaffold (Fig. 5a).

To assess cell morphology and matrix deposition, SEM was performed on the surfaces of scaffolds (Fig. 7). On day 14 of cultivation, a thin sheet of cells and matrix covered the scaffolds (Fig. 7a), a net structure formed in 3D cultures, which not only connected most of the ADSCs but also extended toward the scaffolds and formed physical connections between ADSCs and the scaffolds (Fig. 7a, b).

We also examined the expression of surface markers CD29, CD44, CD34, CD45, CD73, CD105, CD166 and HLA-DR of ADSCs cultured with the two methods by flow cytometry. CD29, CD44, CD13, CD105 and CD166 were positive expression, while CD34, CD45, and HLA-DR were negative (Fig. 8). The positive expression ratios of the two kind of expanded cells had no significant difference.

The expression of transcription factors which represent multi-differentiation ability, such as Oct-4, Sox-2 and Rex-1 was also examined for the expanded cells. The Oct-4, Sox-2 and Rex-1 mRNA expression of ADSCs in scaffold was higher than that in plate ($P < 0.05$) (Fig. 9a, b).

The differentiation potential of the ADSC was evaluated by histochemistry staining (Fig. 10). After 14 days

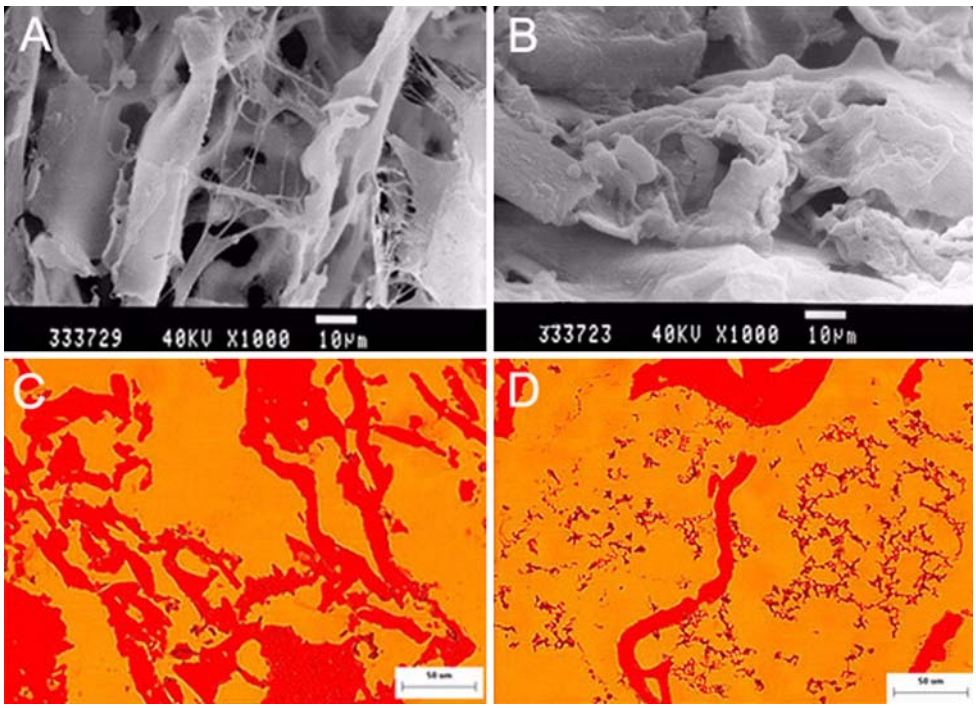

Fig. 4 Up: SEM images of ADSCs growing in collagen–chitosan scaffolds; **a** (7:3) × 800, **b** (5:5) × 1000. Down: Images of ADSCs growing on collagen–chitosan scaffolds with HE stain. **a** (7:3), **b** (5:5) × 200

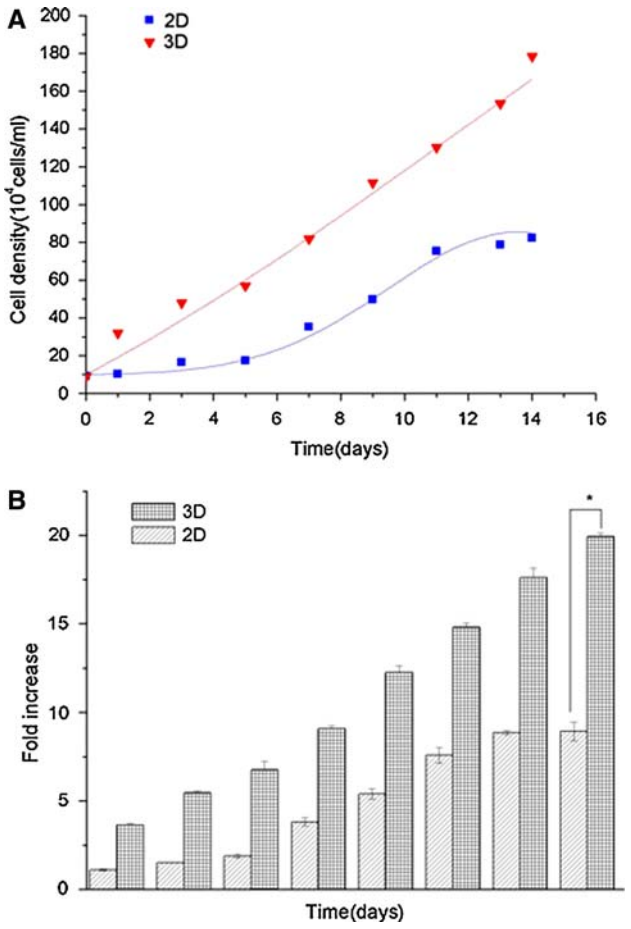

Fig. 5 Growth dynamics of ADSCs in 2D and 3D microenvironment. **a** The growth curve of ADSCs. **b** Expansion fold of total expanded cells. $^*P < 0.05$

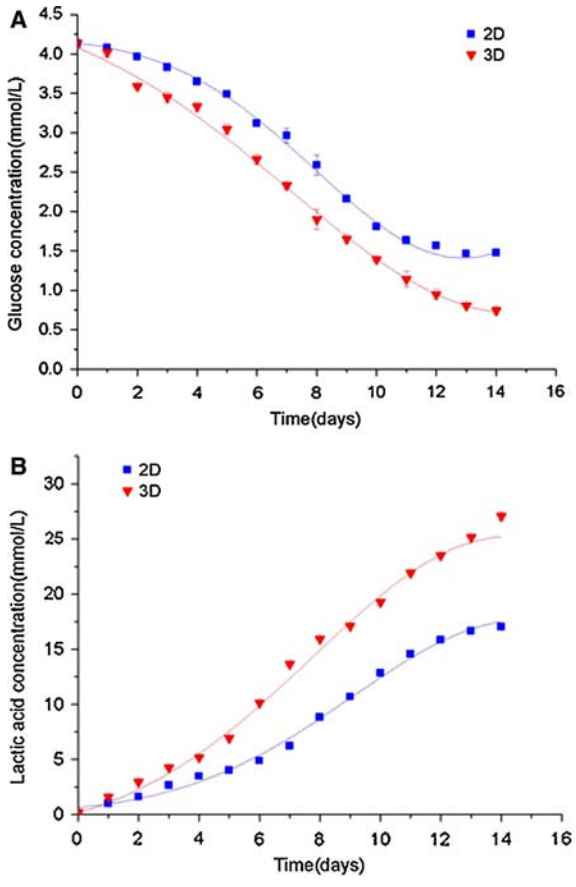

Fig. 6 Changes of glucose and lactic acid concentration during culture period. Glucose (**a**) and lactate acid (**b**). Values displayed represent the average of three independent experiments

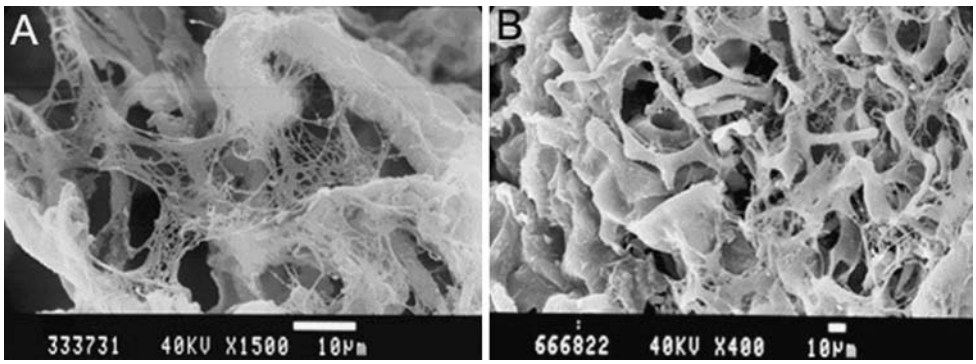

Fig. 7 Scanning electron microscopy of ADSCs in scaffolds

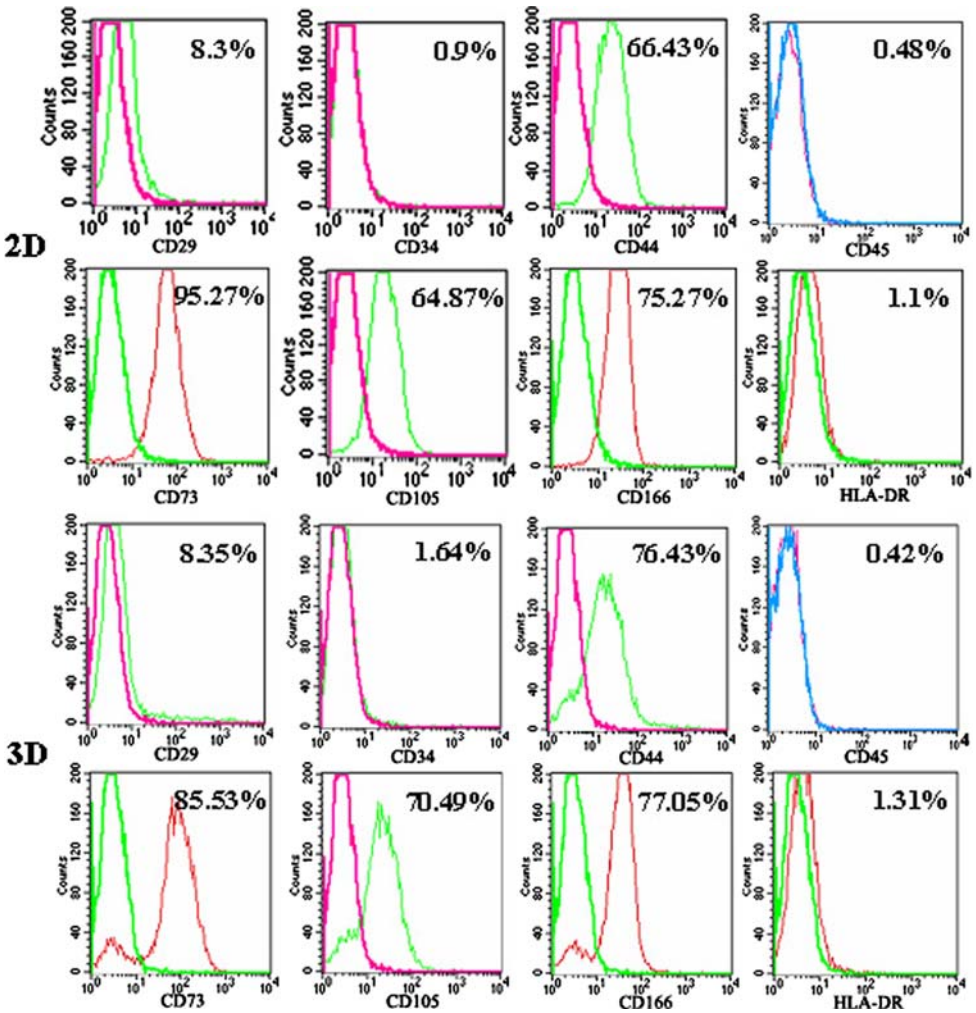

Fig. 8 Expression of stem cell relative surface markers of expanded ADSCs in 2D and 3D cultures. **a** Flow cytometry analysis shows the surface immunophenotype of ADSCs in each culture system. **b** Expression levels of each phenotype in expanded ADSCs in each culture system ($P > 0.05$)

expansion, cells and cells–scaffold complexes were induced toward the adipogenic, chondrogenic and osteogenic cell lineage. Oil Red O staining, Toluidine blue staining and von Kossa staining indicated that the expanded ADSCs in scaffold also have strong multi-differentiation ability (Fig. 10d–f), almost the same as ADSCs cultured in plate (Fig. 10a–c). The results of histochemistry staining also identified the multi-differentiation ability of expanded cells further, and consistent with the results of RT-PCR.

4 Discussion

Tissue engineering approach, which consists of an interactive triad of responsive cells, supportive matrix, and

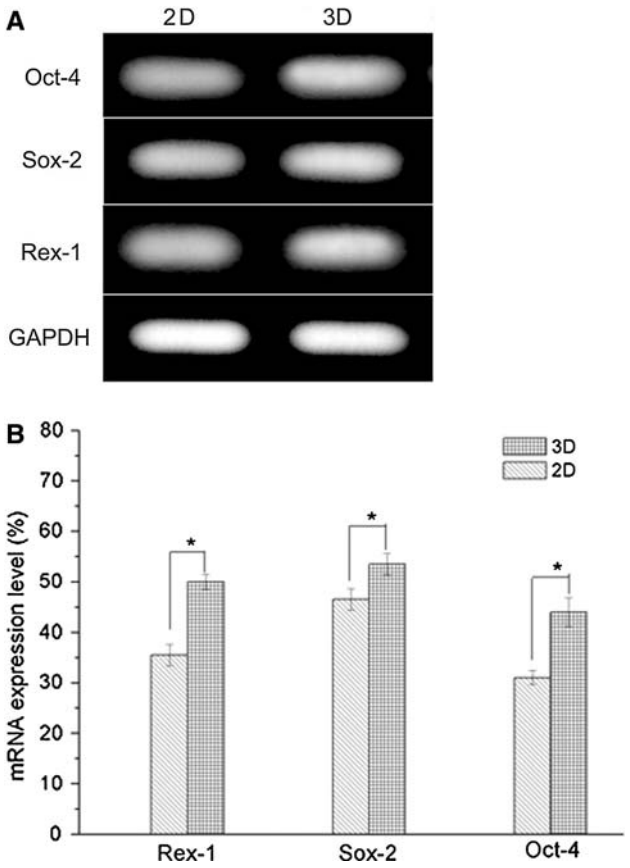

Fig. 9 Transcription factors mRNA expression of expanded ADSCs. **a** Total cellular RNA was analyzed by RT-PCR for Oct-4, Sox-2 and Rex-1 mRNA expression. **b** Semi-quantitative analysis of RT-PCR results. $*P < 0.05$

bioactive molecules, utilizes both engineering and life science discipline to promote organ or tissue regeneration and to sustain, recover their functions [1, 22, 23]. A three-dimensional scaffold provides an extra cellular matrix analog which functions as a necessary template for host infiltration and a physical support to guide the proliferation and differentiation of cells into the targeted functional tissue or organ [14, 24]. The optimal scaffold should support the movement, proliferation, and differentiation of specific cells.

The biomaterials (collagen and chitosan) used in this work are of natural origin, and especially collagen is an integral component in the human physiological structures. However, because of the fast biodegrading rate and the low mechanical strength, chitosan was added. One of the important purposes adding chitosan is providing additional amino groups which function as binding cites with collagen to improve the stability of the collagen without significantly altering the chemical characteristics of the both polymers. Therefore, the interpenetration of collagen and chitosan in the scaffold is crucial.

It is known that the microstructure properties such as pore size and its distribution, porosity as well as pore shape all have prominent influence on cell intrusion, proliferation and function in tissue engineering [12, 20]. The results indicate that the morphology difference is mainly caused by rehydration and relyophilization process in the EDC cross-linking treatment. This additional refreeze-drying can induce the collagen fibers to be combined again to form sheets, leading to the fusion of some smaller pores to

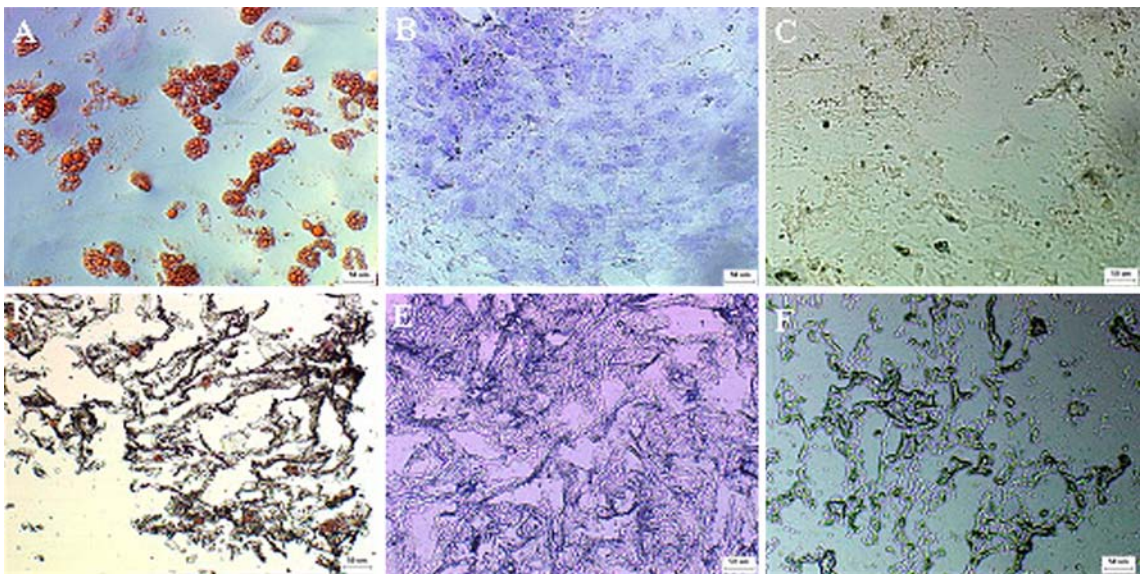

Fig. 10 Multi-differentiation of expanded ADSCs. ADSCs were induced toward adipocytes (**a**, **d**), chondrocytes (**b**, **e**) and osteocytes (**c**, **f**). **a**–**c** ADSCs expanded in 2D. **d**–**f** ADSCs expanded in 3D

generate larger ones. It has to be noted that the slight collapse of the scaffold during this process can reduce the pore size. On the other hand, this collapse, if not occurs homogeneously in 3D, will inevitably produce elongated pores as shown in Fig. 2c. Because of the suitable pore size for the growth of cell in scaffold is 50–200 μm, so the scaffolds with the collagen–chitosan ratio of 9:1, 7:3 and 5:5 can be used for cell culture.

The water-binding ability, another important factor influencing the proliferation of cells in scaffold, could be attributed to their hydrophilicity and the maintenance of their 3D structure. In general, the water content is decreased after cross-linking because of the decrease of the hydrophilic groups [25]. As mentioned above, the collapse during the refreeze-drying procedure will cause the reduction of the porosity, hence, the decrease of bibulous ability and water content. However, the interval porosities of our scaffolds are all exceed 90% and the absolute value of water content is still over 80 times of its initial weight after EDC treatment, which are high enough for tissue engineering [26]. When the scaffolds are capable of swelling they allow their pore size to increase in diameter in order to swell thus facilitating the cells not only to attach but also to penetrate inside the scaffold to grow in a three-dimensional pattern. Moreover the cells avail the maximum internal surface area of the scaffold. Since cross-linked scaffolds of 7:3 and 5:5 show maximum percentage of bibulous ability than any other scaffolds, it is obvious that they can avail nutrients of the culture media more effectively during in vitro culture.

The stability of scaffold is important in tissue engineering. The presence of chitosan can obviously improve the biostability of the collagen–chitosan scaffold, and the ability to resist collagenase degradation was further enhanced by EDC cross-linking. Cross-linking of the collagen-based scaffolds is an effective method to modify the biodegrading rate and to optimize the mechanical property [17, 27]. EDC has become popular as a cross-linking reagent for collagen-based biomaterials [28, 29]. EDC cross-links collagen molecules by the formation of isopeptides without being incorporated itself, thus precluding depolymerization and possible release of potentially cytotoxic reagents [17, 30]. Furthermore, the by-product of the cross-linking reaction is urea [31], which has no cytotoxicity and can be easily removed during routine rinsing of the matrices. Cross-linked collagen–chitosan sponges reveal that cross-linking produces noconsiderable alterations to scaffold morphology but distinct changes to scaffold stability and mechanical property. Cross-linked scaffolds with high concentration of chitosan showed better biostability than those non-cross-linked, and the biostability was increased with the increase of chitosan concentration.

Comprehensively considering pore size, bibulous ability, interval porosity and biodegradation of all kinds of scaffolds, we chose the scaffolds of 7:3 and 5:5 volume ratios to analyze the biocompatibility with ADSC. Chitosan-combined and EDC-treated scaffold preserves the original good cytocompatibility of collagen. Because cell infiltration and proliferation are crucial for a scaffold to support and guide tissue regeneration, we observed the infiltration and proliferation of ADSCs by SEM and H&E staining. Our developed scaffold with volume ratio 7:3 has better cytocompatibility than that of 5:5. This mainly because collagen has better biocompatability with cells than chitosan, and suitable for cell attachment and proliferation.

Since scaffold provided more area in 3D space, the cell density was over 2×10^6 cells/ml after 14 days culture of ADSCs in collagen–chitosan scaffold, the cell number increased up to 26-fold, which was obviously higher than that in 2D. On the basis of its morphological characters, we suppose that this structure is composed of cells and extracellular matrix proteins which play an important role in cell–cell and cell–scaffold interactions [5]. Thus the proteins promoted the signal transduction for efficient ADSC expansion. This may be the part of reasons for the considerable proliferation of ADSC in scaffolds.

What's more, even the concentration of lactic acid is above 20 mM after 9 days incubation of ADSCs in scaffolds, an extended exponential growth phase was still observed. While in 2D, the growth and metabolism of ADSCs were nearly inhibited by the end of the experimental period. Some studies indicated that the proliferation will be inhibited when lactate concentration is above 20 mM [32, 33]. However, because of the unique properties of 3D scaffold-based cell cultures, loading capacities for growth or inhibitive factors [34], 20 mM lactate concentration is no longer the inhibitory for ADSC growth in 3D environment.

Whether the expanded ADSCs in collagen–chitosan scaffolds still remained their stem cell characteristics is another important issue. As we all know, mesenchymal stem cells are characterized by their fibroblastic cell morphology, their high expansion capacity in vitro, and their expression of typical cell surface markers, their potential to avoid allogenic rejection after transplantation, and their pronounced differentiation potential into distinct mesenchymal tissues [35]. Stem cell relative surface markers CD29, CD44, CD13, CD105 and CD166 [36–38] of expanded cells in 3D were positive expression. Meanwhile all expanded cells positively expressed Oct-4, Sox-2 and Rex-1 mRNA, which play important role in differentiation potentials of stem cells [39, 40]. It suggested that the expanded cells remained their multi-differentiation potency. Furthermore, based on the histological staining, the differentiation potential of the cells after expansion was

successfully demonstrated by their adipogenesis, osteogenesis and chondrogenesis. Therefore, the prerequisite for in vitro expansion of ADSCs is accomplished by maintaining the differentiation potential.

According to the above characteristics of collagen–chitosan scaffold, we can see that it is a promising scaffold for tissue engineering with ADSC. We have applied this scaffold to expand ADSCs, and constructe an engineered cardiac tissue with ADSCs. ADSCs grew in the scaffold very well, expanded cells can easily be collected from scaffold and still remianed the characteristics of stem cells and multi-differentiation ability. We also successfully differentiate ADSCs into cardiomyocytes in the scaffold. (These papers have not published yet.) All these experiments demonstrated that our fabricated scaffold suitable for the proliferation and differentiation of ADSCs, and can be use for cell expansion and tissue engineering.

5 Conclusions

Our developed collagen–chitosan scaffolds have suitable pore size, interval porosity, bibulous ability, biodegradation and good biocompatibility with ADSCs, and can effectively support and accelerate the proliferation and differentiation of ADSCs.

Acknowledgments This work was supported by The National Natural Sciences Foundation of China and Young Teacher Culture Foundation of Dalian University of Technology.

References

1. Y.F. Zhang, X.R. Cheng, J.W. Wang et al., Biochem. Biophys. Res. Commun. **344**, 362 (2006). doi:10.1016/j.bbrc.2006.03.106
2. T. Ueda, K. Tsuji, H. Yoshino et al., J. Clin. Invest. **105**, 1013 (2000). doi:10.1172/JCI8583
3. P.A. Sotiropoulou, S.A. Perez, M. Salagianni et al., Stem Cells **24**, 462 (2006). doi:10.1634/stemcells.2004-0331
4. Y.-x. Zhu, T.-q. Liu, K.-d. Song et al., Cell Biochem. Funct. **26**, 664 (2008)
5. H. Liu, K. Roy, Tissue Eng. **11**, 319 (2005). doi:10.1089/ten.2005.11.319
6. B. Geiger, A. Bershadsky, R. Pankov, K.M. Yamada, Nat. Rev. Mol. Cell Biol. **2**, 793 (2001). doi:10.1038/35099066
7. W. Tan, R. Krishnaraj, T.A. Desai, Tissue Eng. **7**, 203 (2001). doi:10.1089/107632701300062831
8. J. Leor, N. Landa, S. Cohen, Expert Rev. Cardiovasc. Ther. **4**, 239 (2006). doi:10.1586/14779072.4.2.239
9. J. Lin, M.L. Lindsey, B. Zhu et al., J. Tissue Eng. Regen. Med. **1**, 211 (2007). doi:10.1002/term.27
10. A. Bozkurt, G.A. Brook, S. Moellers et al., Tissue Eng. **13**, 2971 (2007). doi:10.1089/ten.2007.0116
11. R.N. Chen, G.M. Wang, C.H. Chen et al., Biomacromolecules **7**, 1058 (2006). doi:10.1021/bm050754b
12. E. Song, S.Y. Kim, T. Chun et al., Biomaterials **27**, 2951 (2006). doi:10.1016/j.biomaterials.2006.01.015
13. E. Donzelli, A. Salvade, P. Mimo et al., Arch. Oral Biol. **52**, 64 (2007). doi:10.1016/j.archoralbio.2006.07.007
14. J.S. Gabbay, J.B. Heller, S.A. Mitchell et al., Ann. Plast. Surg. **57**, 89 (2006). doi:10.1097/01.sap.0000205378.89052.d3
15. B. Wang, J. Han, Y. Gao et al., Neurosci. Lett. **421**, 191 (2007). doi:10.1016/j.neulet.2007.04.081
16. W. Hao, Y.Y. Hu, Y.Y. Wei et al., Cell. Tissue. Organ. **187**, 89 (2008)
17. S. Yunoki, N. Nagai, T. Suzuki, M. Munekata, J. Biosci. Bioeng. **98**, 40 (2004)
18. N. Shanmugasundaram, P. Ravichandran, P.N. Reddy et al., Biomaterials **22**, 1943 (2001). doi:10.1016/S0142-9612(00)00220-9
19. I. Van der Lubben, J.C. Verhoef, G. Borchard, H.E. Junginger, Eur. J. Pharm. Sci. **14**, 201 (2001)
20. L. Ma, C.Y. Gao, Z.W. Mao et al., Biomaterials **24**, 4833 (2003). doi:10.1016/S0142-9612(03)00374-0
21. J. Yan, X. Li, L. Liu et al., Artif. Cells Blood Substit. Immobil. Biotechnol. **34**, 27 (2006). doi:10.1080/10731190500430024
22. M. Kim, Y.S. Choi, S.H. Yang et al., Biochem. Biophys. Res. Commun. **348**, 386 (2006). doi:10.1016/j.bbrc.2006.07.063
23. D.C. Chen, Y.L. Lai, S.Y. Lee et al., J. Biomed. Mater. Res. A **80A**, 399 (2007). doi:10.1002/jbm.a.30932
24. A. Kim, N. Lakshman, W.M. Petroll, Exp. Cell Res. **312**, 3683 (2006). doi:10.1016/j.yexcr.2006.08.009
25. L. Buttafoco, P. Engbers-Buijtenhuijs, A.A. Poot et al., J. Biomed. Mater. Res. B Appl. Biomater. **77B**, 357 (2006). doi:10.1002/jbm.b.30444
26. X. Wang, L. Liu, Q. Zhang, Zhongguo Xiu. Fu Chong. Jian. Wai Ke. Za Zhi. **21**, 120 (2007)
27. H.M. Powell, S.T. Boyce, Biomaterials **28**, 1084 (2007). doi:10.1016/j.biomaterials.2006.10.011
28. S.N. Park, J.C. Park, H.O. Kim, M.J. Song, H. Suh, Biomaterials **23**, 1205 (2002). doi:10.1016/S0142-9612(01)00235-6
29. T. Taguchi, T. Ikoma, J. Tanaka, J. Biomed. Mater. Res. **61**, 330 (2002). doi:10.1002/jbm.10147
30. C.S. Osborne, W.H. Reid, M.H. Grant, Biomaterials **20**, 283 (1999). doi:10.1016/S0142-9612(98)00179-3
31. E. Khor, Biomaterials **18**, 95 (1997). doi:10.1016/S0142-9612(96)00106-8
32. A.M. Fernandes, T.G. Fernandes, M.M. Diogo et al., J. Biotechnol. **132**, 227 (2007). doi:10.1016/j.jbiotec.2007.05.031
33. S.D. Patel, E.T. Papoutsakis, J.N. Winter, W.M. Miller, Biotechnol. Prog. **16**, 885 (2000). doi:10.1021/bp000080a
34. J.L. Williams, J.P. Iannotti, A. Ham, J. Bleuit, J.H. Chen, Biorheology **31**, 163 (1994)
35. J.M. Ryan, F.P. Barry, J.M. Murphy, B.P. Mahon, J. Inflamm. **2**, 8 (2005). doi:10.1186/1476-9255-2-8. (Lond)
36. L. Lei, W. Liao, P. Sheng, M. Fu, A. He, G. Huang, Sci. China C Life Sci. **50**, 320 (2007). doi:10.1007/s11427-007-0019-z
37. M.J. Varma, R.G. Breuls, T.E. Schouten et al., Stem Cells Dev. **16**, 91 (2007). doi:10.1089/scd.2006.0026
38. A. Schaffler, C. Buchler, Stem Cells **25**, 818 (2007). doi:10.1634/stemcells.2006-0589
39. A. Remenyi, K. Lins, L.J. Nissen et al., Genes Dev. **17**, 2048 (2003). doi:10.1101/gad.269303
40. F. Villinger, T. Rowe, B.S. Parekh et al., J. Med. Primatol. **30**, 254 (2001). doi:10.1034/j.1600-0684.2001.d01-57.x